



OPEN

Anticancer effects of pomegranate-derived peptide PG2 on CDK2 and miRNA-339-5p-mediated apoptosis via extracellular vesicles in acute leukemia

Kantorn Charoensedtasin¹, Chosita Norkaew¹, Mashima Naksawat¹, Wasinee Kheansaard¹, Sittiruk Roytrakul² & Dalina Tanyong¹✉

Acute leukemia has rapid onset and severe complications. Anticancer peptides from natural sources have demonstrated efficacy in eliminating various cancers through apoptosis signaling pathways. Additionally, extracellular vesicles containing microRNAs play pivotal roles in promoting tumorigenesis. Therefore, this study aimed to investigate the impact of PG2, a pomegranate peptide that regulates extracellular vesicles, on the induction of acute leukemia cell apoptosis. NB4 and MOLT-4 leukemia cell lines were treated with PG2 alone or in combination with daunorubicin to assess cell viability using the MTT assay. Extracellular vesicles were extracted from PG2-treated NB4 and MOLT-4 cells. Bioinformatic tools were utilized to predict target proteins and microRNAs, following which mRNA and protein expression were determined by using RT-qPCR and western blotting, respectively. PG2 significantly reduced the viability of NB4 and MOLT-4 cells. Furthermore, the combination of PG2 with daunorubicin had a synergistic effect on NB4 and MOLT-4 cells. Subsequent treatment with PG2 or PG2-treated extracellular vesicles decreased CDK2 expression while increasing microRNA-339-5p and caspase-3 expression in NB4 and MOLT-4 cells. Our findings revealed that the anticancer activity of PG2 through the CDK2/miR-339-5p/caspase-3 pathway is mediated by extracellular vesicles, ultimately inducing apoptosis. PG2 holds promise as a potential antileukemic drug.

Keywords Pomegranate, MicroRNA, Extracellular vesicles, Apoptosis, Leukemia

Leukemia is a hematological malignancy characterized by abnormal proliferation of hematopoietic stem cells. Leukemia is one of the top ten most common cancers worldwide¹. Leukemia can be divided into 4 main types: acute myelocytic leukemia, acute lymphocytic leukemia, chronic myelocytic leukemia and chronic lymphocytic leukemia. Acute leukemia is defined as a rapid-onset and aggressive type of leukemia that features severe complications in patients. Acute leukemia disease can be treated by several approaches, such as chemotherapy, radiotherapy, or targeted therapy. However, adverse effects from chemotherapy can cause the suffering of leukemia patients during treatment and the possibility of chemoresistance. Moreover, the discovery of new treatment approaches is necessary to increase recovery from leukemia². Bioactive compounds from natural sources could be an alternative treatment. Several anticancer peptides (ACPs) isolated from natural sources suppress cancer progression via specific mechanisms with low toxicity to normal cells and reduce drug resistance. ACPs usually contain 5–50 amino acids and are hydrophobic, resulting in easy penetration through the cell membrane^{3–5}. Interestingly, the structure of ACPs can be modified to improve their pharmacokinetic and pharmacodynamic properties. Previous studies have demonstrated that *Punica granatum* (pomegranate) extract from various parts of the fruit, as well as its most abundant compound, punicalagin, can induce cell death and reduce tumorigenesis via various signaling pathways^{6–8}. Unidentified compounds from pomegranate

¹Department of Clinical Microscopy, Faculty of Medical Technology, Mahidol University, 999 Phuttamonthon sai 4 Road, Salaya, Phuttamonthon, Nakhon Pathom 73170, Thailand. ²Functional Proteomics Technology Laboratory, Functional Ingredients and Food Innovation Research Group, National Center for Genetic Engineering and Biotechnology, National Science and Technology for Development Agency, Pathum Thani 12120, Thailand. ✉email: dalina.itc@mahidol.ac.th

could be effective cancer treatments. Despite the synthesis of pomegranate bioactive peptides for antimicrobial purposes^{9,10}, further development of ACP is necessary within the field of oncology.

MiRNAs are small 21–23 nucleotide fragments of RNA that serve to inhibit the transcription of target genes by binding to 3′ untranslated regions (3′UTRs) of RNA sequences, consequently decreasing gene and protein levels¹¹. Some natural compounds can potentially regulate gene expression via miRNAs¹². Extracellular vesicles (EVs) are heterogeneous particles containing proteins, RNA, and miRNAs that act as mediators between cells. The types of EVs can be classified into exosomes, microvesicles, and apoptotic bodies based on their size and biogenesis. Since EVs consist of several types of miRNAs and proteins, EVs derived from cancer cells could serve as mediators for promoting cancer survival and progression by regulating the microenvironment^{13,14}. In addition, the presence of a chemical in EVs is associated with the survival of cancer cells, leading to drug resistance¹⁵. Some compounds can reverse the ability of EVs to promote tumor cell survival as well as drug resistance¹⁶. Therefore, miRNAs and EVs could serve as targets for leukemia treatment. In this study, we designed pomegranate peptides to study the apoptosis signaling pathway and miRNAs involved in EVs. Moreover, bioinformatics tools have been used to identify the molecules most likely involved in leukemic EV-regulated apoptosis.

Results

PG2 is cytotoxic to NB4 and MOLT-4 cells in a dose-dependent manner

All peptides are shown in Table 1, and peptides at a concentration of 1000 µg/ml were screened against NB4 and MOLT-4 cells using the MTT assay. PG2 had the greatest effect on reducing the viability of the NB4 and MOLT-4 cells, as shown in Fig. 1A. Afterward, MOLT-4 cells were treated with 0, 500, 750–1000 µg/ml PG2 for 24–48 h and analyzed using the MTT assay. According to Fig. 1B and C, the viability of NB4-treated cells was significantly decreased after treatment with 500, 750 and 1000 µg/ml PG2 for 24 h and 48 h, while the viability of MOLT-4-treated cells was significantly decreased after treatment with 750 and 1000 µg/ml PG2 for 24 h and 48 h. Moreover, less cytotoxicity was observed in healthy PBMCs, as shown in Fig. 1D. The IC₅₀ values of PG2 for NB4 and MOLT-4 cells at 24 h were 656 ± 6.0 and 640 ± 6.0 µg/ml, respectively, while those at 48 h were 581 ± 4.2 and 612 ± 3.1 µg/ml, respectively. In summary, PG2 was selected as an antileukemic peptide and inhibited NB4 and MOLT-4 cells in a dose-dependent manner.

The combination of PG2 and daunorubicin had synergistic effects on NB4 and MOLT-4 cells

The effect of the combination of PG2 and daunorubicin, which is a chemotherapeutic drug for leukemia disease, was investigated using the MTT assay. PG2 combined with daunorubicin significantly decreased the percentage of viable NB4 and MOLT-4 cells compared to the control, daunorubicin alone and PG2 alone, as depicted in Fig. 2A. Additionally, the combination index (CI) was calculated by CompuSyn. The combination index plot of PG2 combined with daunorubicin in NB4 and MOLT-4 cells is shown in Fig. 2B. The average CIs of PG2 and daunorubicin were 0.98 and 0.94 for NB4 and MOLT-4 cells, respectively. In summary, the combination of PG2 with daunorubicin had a synergistic effect on NB4 and MOLT-4 cells.

PG2-induced expression of the target proteins CDK2 and mir-339-5p in leukemic EVs

Due to the limited ability of SwissTargetPrediction to predict target proteins from PG2, which comprises 12 amino acids, the PG2 peptide for predicting target proteins was divided into 2 parts: LLKLFF and PFLKTG. The possible candidate target proteins of PG2 included 76 proteins (Fig. 3A), as depicted in Supplementary table S1. The proteomic profile of leukemic EVs from previous studies revealed 1301 proteins, as depicted in Supplementary table S2. As shown in Figs. 3B and 11 target proteins in EVs were identified and investigated for protein–protein interactions. The STRING database revealed that all target proteins interact with representative proteins involved in apoptosis, including caspase-3, caspase-8 and caspase-9, as depicted in Fig. 3C. The only proteins that interact with 3 caspase families were CTSD, CAPN1, MAPK1, CDK2 and HDAC1. The probability of association of each target protein and the divided PG2 sequence (LLKLFF and PFLKTG) was determined, as shown in the heatmap in Fig. 3D. The gene with the highest probability score (0.05918) was CDK2. Therefore, CDK2 was a candidate protein in this study.

In part of the miRNA prediction, the sequence protein of CDK2 (ENSG00000123374) retrieved from the NCBI database was used to predict candidate miRNAs from the TargetScan, miRDB and DIANA databases. miRNA profiles of leukemic EVs were obtained from the EVmiRNA database (<http://bioinfo.life.hust.edu.cn/EVmiRNA>). Seventeen PG2-responsive miRNAs were predicted from the miRDB, and eighteen miRNAs were predicted from the TargetScan and DIANA databases. According to Fig. 3E, miRNAs in leukemic EVs predicted by the TargetScan and miRDB databases were not found, while miRNAs in leukemic EVs predicted by the DIANA database were hsa-miR-339-5p, for which miTG = 0.907. Therefore, hsa-miR-339-5p was a candidate miRNA in this study.

Peptide name	Amino acid sequences	Net charge	pI	Hydrophobicity (%)	Structure Prediction
PG1	LLKLFFPFLKLG	0	6.97	66.67	CCCCCHCCCC
PG2	LLKLFFPFLKTG	+2	10.66	66.67	CCCCCCCCCCCC
PG3	LKLFFPFLRT	+2	11.56	70	CCCHCHHCCC
PG4	LRLFFPFLRT	+2	12.49	70	CCCHCHHCCC

Table 1. List of Pomegranate derived peptides. L: leucine, K: lysine, P: proline, E: glutamic acid, T: threonine, G: glycine, R: arginine.

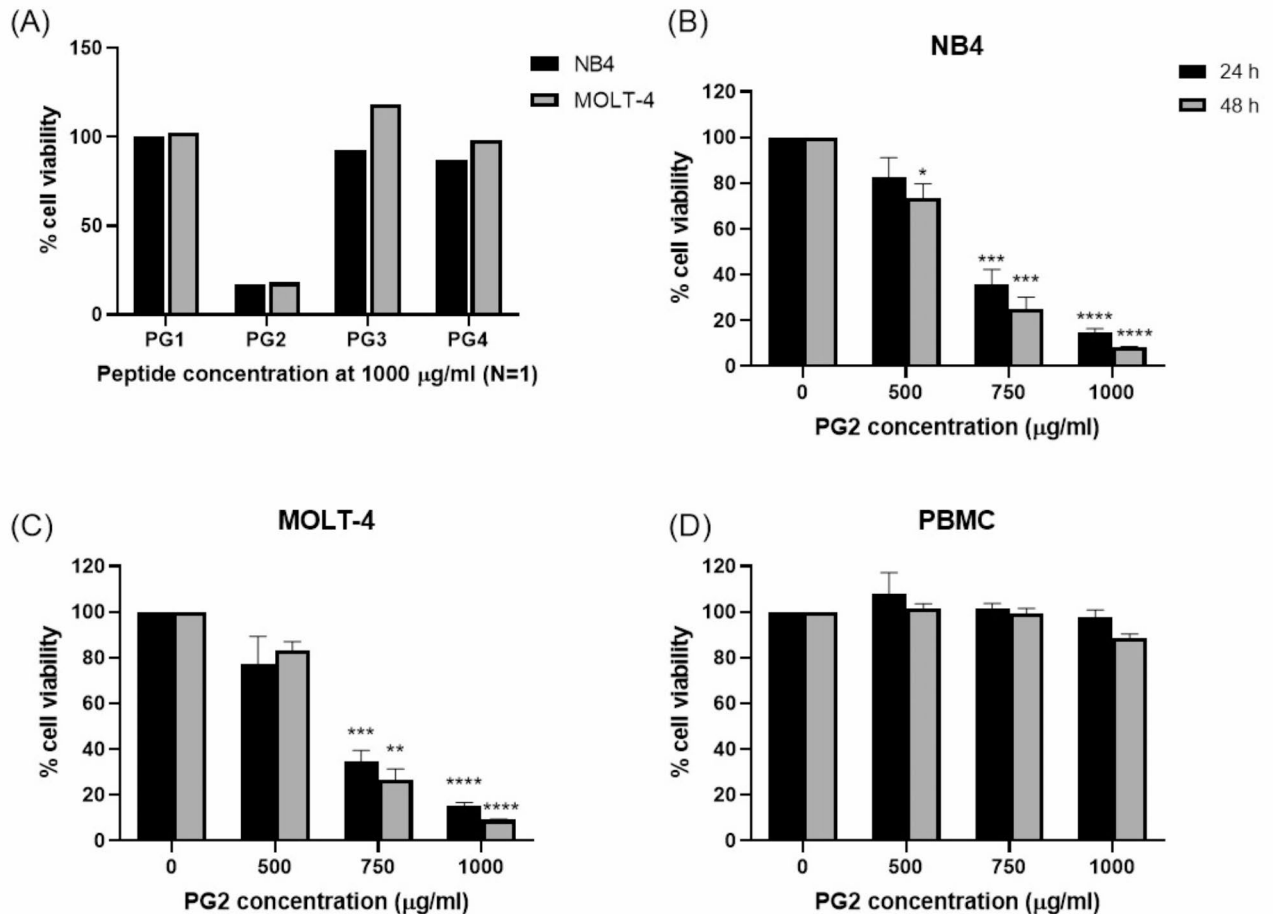


Fig. 1. The inhibitory effect of PG2 on cell viability of NB4 and MOLT-4 cells. **(A)** Screening for the inhibitory effect of 1000 µg/ml of PG1, PG2, PG3 and PG4 at 24 h analyzed using MTT assay. Various concentrations of PG2 were used to treat in **(B)** NB4, **(C)** MOLT-4 and **(D)** PBMC at 24 and 48 h analyzed using MTT assay. Data were represented as mean \pm S.E.M of three independent experiments. Statistical comparison was performed using student t-test. * $p < 0.05$, ** $p < 0.01$, *** $p < 0.001$, and **** $p < 0.0001$ were considered as statistically significant difference compared to 0 µg/ml PG2.

PG2 induces apoptosis in NB4 and MOLT-4 cells via CDK2, caspase-3, and miR-339-5p

To determine the effect of PG2 on the induction of apoptosis, PG2-treated NB4 and MOLT-4 cells were stained with FITC-conjugated Annexin V and propidium iodide (PI). Figure 4A showed that the total percentage of apoptotic cells in PG2-treated NB4 and MOLT-4 cells was significantly greater than that in untreated NB4 and MOLT-4 cells. Moreover, the cell cycle distribution of PG2-treated NB4 and MOLT-4 cells was investigated using flow cytometry. The proportion of PG2-treated cells in the sub-G1 phase was significantly greater than that in the control group, as shown in Fig. 4B.

Caspase-3, which is a main executioner caspase in apoptosis signaling, was assessed. According to previous bioinformatic studies, CDK2 and miR-339-5p expression was also assessed. As shown in Fig. 5A, compared with no treatment, PG2 significantly decreased the expression of the caspase-3 gene but increased the expression of the CDK2 and miR-339-5p genes in NB4 and MOLT-4 cells. Furthermore, caspase-3 and CDK2 protein expression in NB4 and MOLT-4 cells was also investigated by western blot. Figure 5B shows that compared with no treatment, PG2 significantly increased caspase-3 protein expression but decreased CDK2 protein expression in NB4 and MOLT-4 cells. Therefore, PG2 induces apoptosis via caspase-3, CDK2 and miR-339-5p in NB4 and MOLT-4 cells.

PG2_EV induced apoptosis regulated by CDK2, caspase-3, and miR-339-5p

To investigate how PG2-treated EVs (PG2_EVs) induce apoptosis in leukemic cells, NB4 and MOLT4 cells were exposed to PG2_EVs, and the percentages of apoptotic and signaling molecules were determined. Both untreated-EVs (Con_EVs) and PG2-treated EVs (PG2_EVs) were between 0.22 and 1.35 µm in size and were positive for the Annexin V, CD9 and CD63 markers (Fig. 6A). After NB4 and MOLT-4 cells were treated with PG2_EVs for 48 h, the total number of apoptotic NB4 and MOLT-4 cells was significantly greater than that after

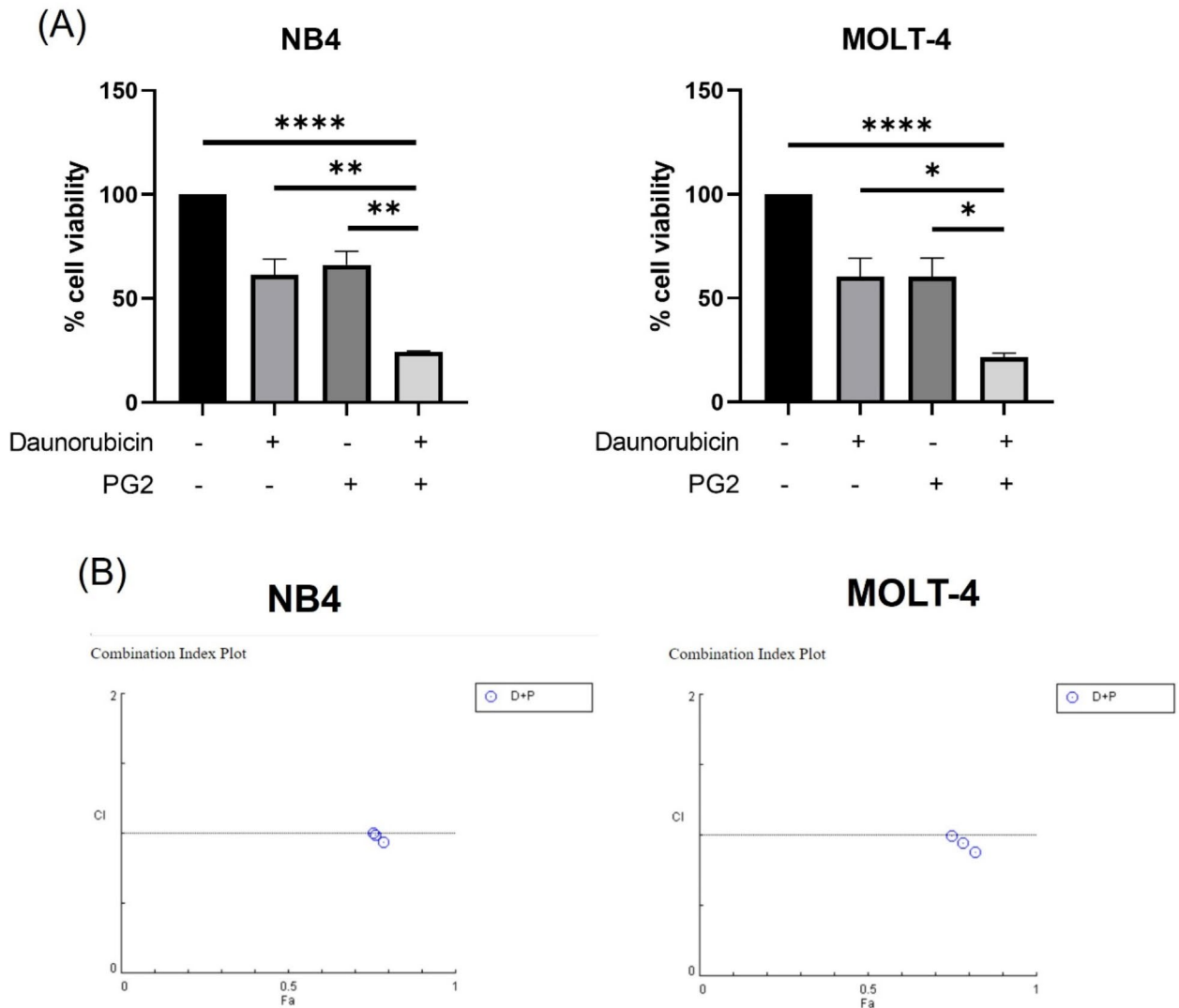


Fig. 2. Synergistic effect of PG2 combination with daunorubicin in NB4 and MOLT-4 cells. **(A)** The effect of combining PG2 with daunorubicin on cell viability of NB4 and MOLT-4 analyzed using MTT assay. **(B)** The combination index plot demonstrated the combination index (CI) of combining PG2 with daunorubicin analyzed using CompuSyn application. Data were represented as mean \pm S.E.M of three independent experiments. Statistical comparison was performed using student t-test. * $p < 0.05$, ** $p < 0.01$, *** $p < 0.001$, and **** $p < 0.0001$ were considered statistically significant difference compared to control, daunorubicin alone and PG2 alone. Fa (fraction affected) indicated inhibitory effect of PG2 combination with daunorubicin of three independent experiments.

treatment with Con_EVs (Fig. 6B). After that, the gene and protein expression levels of caspase-3, CDK2 and miR-339-5p were also determined using RT-qPCR and western blotting, respectively. As shown in Fig. 6C and D, caspase-3 gene and protein expression were significantly greater in both NB4 and MOLT-4 cells treated with PG2_EVs at 48 h than in those treated with Con_EVs. In contrast, PG2_EVs significantly decreased CDK2 gene and protein expression. Moreover, miR-339-5p was increased in both NB4 and MOLT-4 cells at 48 h compared to that in Con_EVs. These results indicated that PG2_EVs increase the expression of miR-339-5p and caspase-3 while decreasing the expression of both the CDK2 gene and protein. Additionally, PG2_EVs may induce miR-339-5p to inhibit CDK2, resulting in the induction of apoptosis in NB4 and MOLT-4 cells.

Discussion

Acute leukemia causes many severe complications in patients, such as disseminated intravascular coagulation (DIC)¹⁷. Moreover, acute leukemia patients frequently develop chemotherapy resistance. Accordingly, there are various treatment approaches, including complementary alternative medicine utilizing natural products. Our study aimed to identify a novel candidate anticancer peptide (ACP) sourced from natural compounds recognized for its effectiveness in cancer therapy while exhibiting minimal cytotoxicity toward normal cells^{3,18,19}.

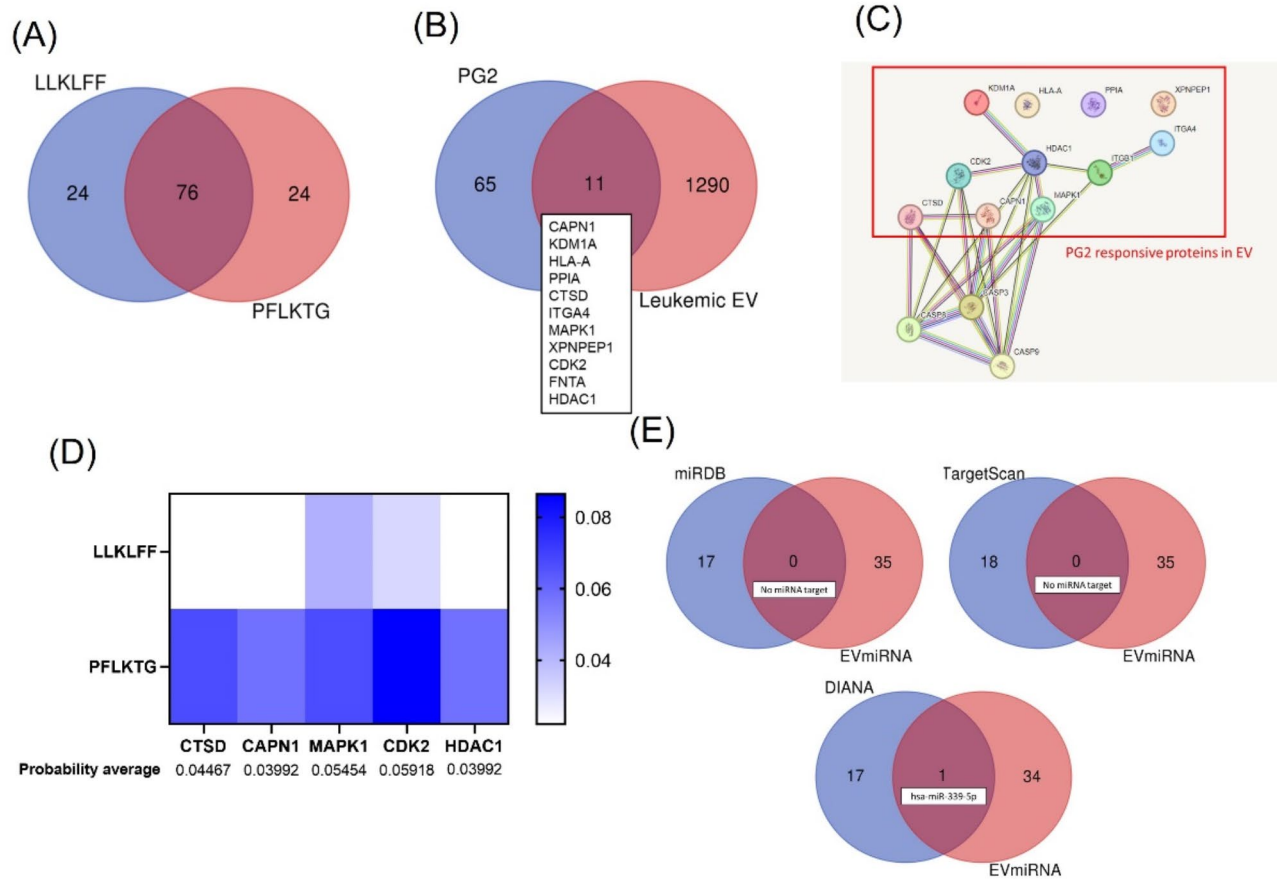


Fig. 3. Target proteins, CDK2, and miR-339-5p in EVs induced by PG2 using bioinformatic analysis. **(A)** Venn-diagram of PG2 responsive proteins from combination between LLKLFF and PFLKTG from PG2. **(B)** Venn-diagram of target proteins from combination between PG2 responsive proteins and leukemic EVs originated from public data. **(C)** A protein-protein interaction of target proteins and apoptotic proteins including caspase-3, caspase-8 and caspase-9 constructed by STRING where red box is PG2 responsive proteins in EVs. **(D)** Heatmap of average probability interaction score between PG2 responsive proteins in EVs which involved in apoptosis and sequence of LLKLFF and PFLKTG in PG2. **(E)** A Venn-diagram between miRNAs predicted from the sequence protein of CDK2 in EVs using three databases (miRDB, DIANA and TargetScan), and miRNAs from EVmiRNA, a database of miRNA profiling in leukemic EVs.

ACPs contain 5–50 amino acids and can induce cancer cell death. Numerous ACPs have been utilized across various cancer types. For instance, LL-37, a cathelicidin peptide, was demonstrated to have anticancer effects on Jurkat T leukemia cells through the activation of the apoptosis signaling pathway²⁰. Similarly, Mustafa E. et al. illustrated the anticancer activity of CM11, which promoted greater levels of apoptosis in Jurkat and Raji cells than in PBMCs²¹. According to previous reports, several bioactive compounds from pomegranate, such as punicalagin⁶ and punicalin²² exhibit anticancer activity through different signaling pathways²³. Hence, undiscovered bioactive peptides from pomegranate could present intriguing options for cancer cell elimination.

In a recent study, PG2 significantly reduced the viability of NB4 and MOLT-4 cells in a dose-dependent manner. Furthermore, combining PG2 with daunorubicin had a synergistic effect on these cells. The unique structure of PG2 includes lysine (K), threonine (T) and glycine (G) amino acid residues, which distinguish it from the other peptides listed in Table 1 and may cause cell death in acute leukemia. Previous reviews have suggested that lysine (K) increases the positive charge within peptides, while glycine (G) interacts with the cell membrane, potentially disrupting its integrity and inhibiting NB4 and MOLT-4 cells^{24,25}.

Bioinformatic tools were utilized to identify target proteins of PG2, revealing Cyclin-dependent kinase 2 (CDK2) and miR-339-5p as molecules involved in apoptosis and extracellular vesicles (EVs). A recent study showed an increase in apoptotic cells and sub-G1 cells in PG2-treated NB4 and MOLT-4 cells. Furthermore, our findings revealed a significant decrease in CDK2 expression, along with significant increases in caspase-3 and miR-339-5p expression, upon treatment with PG2 in NB4 and MOLT-4 cells. CDK2 is an enzyme that is crucially involved in the induction of cell cycle progression from the G1 phase to the S phase. Numerous studies have utilized CDK2 as a therapeutic target. For instance, propofol, an intravenous anesthetic, was used to inhibit the growth of bladder cancer cells by regulating the miR-340/CDK2 axis²⁶. Similarly, Chao Z. et al. demonstrated

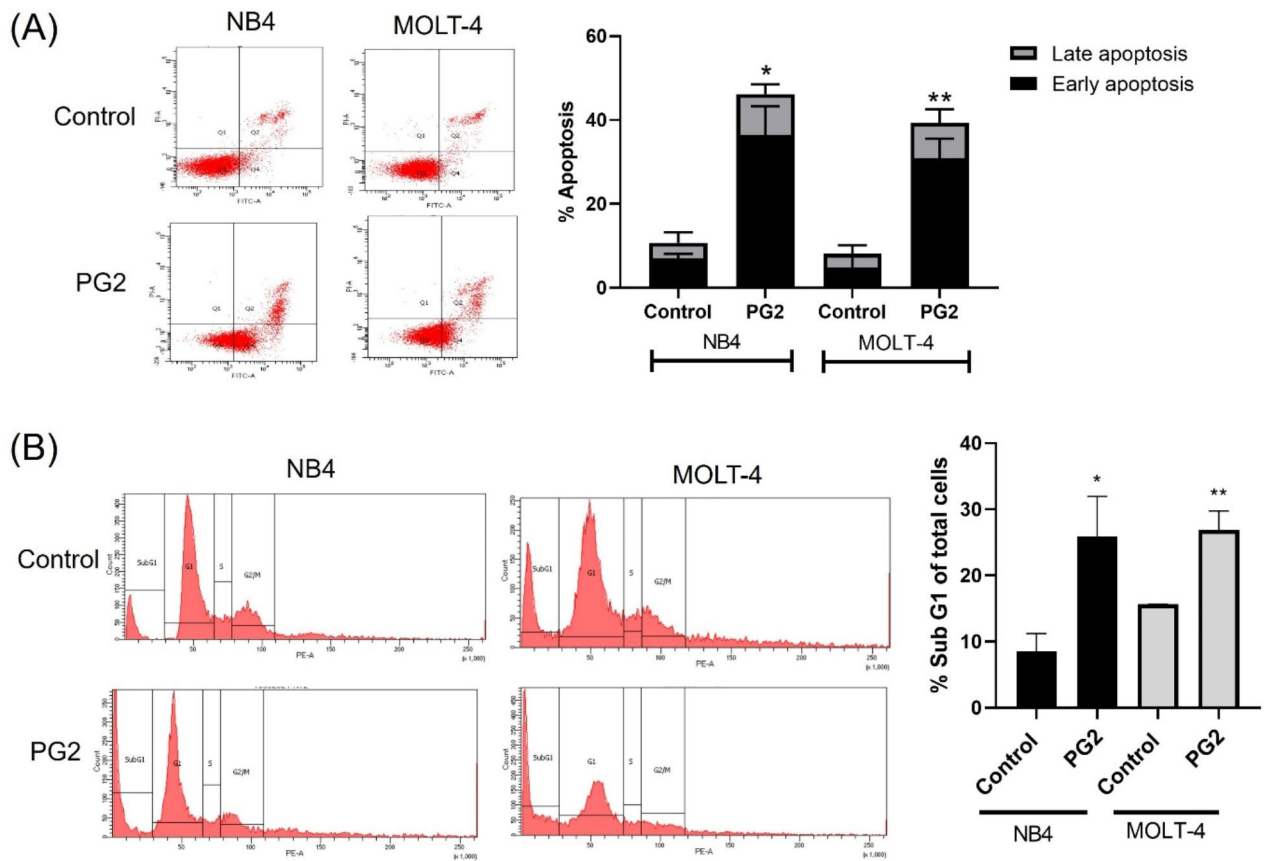


Fig. 4. Apoptosis induction by PG2 in NB4 and MOLT-4 cells. NB4 and MOLT-4 cells were treated with IC50 of PG2 at 48 h. After that, apoptotic cells and cell cycle were analyzed by flow cytometry. **(A)** Flow cytometry scatter plot of Annexin V and PI staining NB4 and MOLT-4 cells and percentage of apoptosis. **(B)** Histogram of cell cycle of NB4 and MOLT-4 cells and percentage of sub G1 of total cells. Data were represented as mean \pm S.E.M of three independent experiments. Statistical comparison was performed using student t-test. * $p < 0.05$ and ** $p < 0.01$ were considered statistically significant difference compared to control.

the anticancer activity of icaritin, a Chinese herbal medicine from barrenwort, in PLC and HT-29 cells, which caused cell cycle arrest and apoptosis by targeting CDK2²⁷.

Many studies have investigated miRNAs as targets for cancer treatment. Interestingly, several natural compounds serve as regulators of miRNAs in signaling pathways^{12,28}. MiR-339-5p was reported to be a tumor suppressive miRNA, and the expression of miR-339-5p was decreased in cancer tissue compared to normal tissue²⁹. There is supported evidence of the association of miR-339-5p and CDK2 in the progression of ER-positive breast cancer³⁰. Additionally, miR-339-5p was reported to be a direct target of proapoptotic genes, including the BCL2L1 and BAX genes, ultimately inducing apoptosis³¹. Caspase-3, which is a well-known executioner caspase in the apoptosis signaling pathway³², was also investigated. In this study, caspase-3 was significantly increased in NB4 and MOLT-4 cells treated with PG2. These results confirmed the effect of PG2 on apoptosis induction via CDK2, miR-339-5p and caspase-3 in NB4 and MOLT-4 cells.

Moreover, the role of EVs derived from PG2-treated leukemic cells (PG2_EVs) in cell communication was investigated. Under normal conditions, leukemic EVs play roles in promoting tumor progression by transferring oncogenes or oncoproteins to different destinations, such as leukemic cells or the microenvironment, which supports tumor cell growth^{13,33}. Wei Yan et al. demonstrated that EVs carrying miR-181b-5p from acute lymphocytic leukemia (ALL) patients promoted the progression of ALL cells by inhibiting apoptosis³⁴. In a previous report, miR-339-5p-containing EVs, which are radiosensitizing miRNAs, were downregulated in esophageal squamous cell carcinoma (ESCC)³⁵. Certain stimuli or conditions have the potential to counteract the effects of tumor-derived extracellular vesicles (EVs) by suppressing their activities. Compared with Con_EV, PG2_EVs induced apoptosis through the modulation of CDK2, miR-339-5p and caspase-3 in NB4 and MOLT-4 cells. PG2_EV may facilitate the transfer of miR-339-5p to suppress CDK2 in adjacent leukemic cells. A previous study revealed that exosomes enriched with miR-21 released from curcumin-treated K562 cells inhibit angiogenesis in HUVECs by targeting RhoB³⁶. Additionally, anticancer SMR peptides can potentially inhibit the growth of tumor cells by blocking the release of EVs and decreasing the levels of Mortalin and C9 in tumor cell lines³⁷. This recent study aligns with previous research indicating that natural compounds and ACP can reduce tumorigenesis and promote apoptosis by enhancing the ability of tumor-derived EVs. However, this

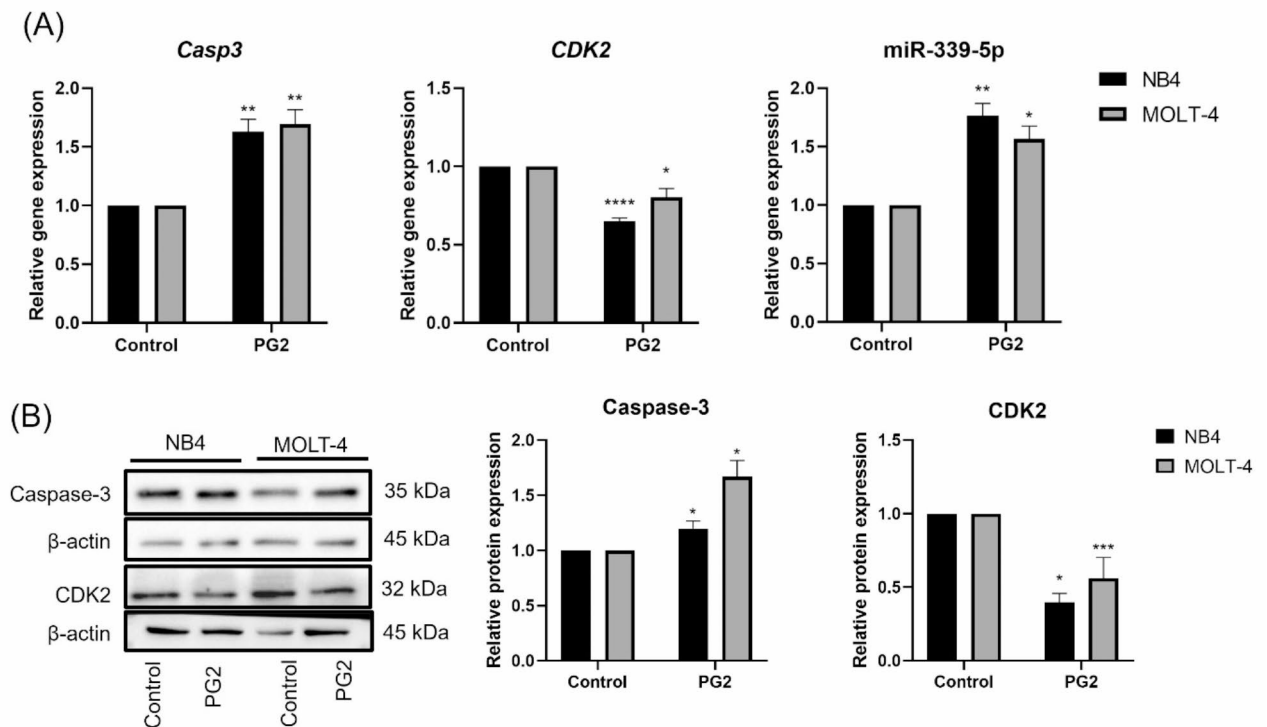


Fig. 5. Effect of PG2 on caspase-3, CDK2 and miR-339-5p expression in NB4 and MOLT-4 cells. NB4 and MOLT-4 cells were treated with IC₅₀ of PG2 at 48 h. Afterward, caspase-3, CDK2 and miR-339-5p in NB4 and MOLT-4 were determined using RT-qPCR and western blotting. **(A)** The mRNA expression of Casp3, CDK2 and miR-339-5p in PG2-treated NB4 and MOLT-4. **(B)** The protein expression of caspase-3 and CDK2 in PG2-treated NB4 and MOLT-4 cells. Data were represented as mean \pm S.E.M of three independent experiments. Statistical comparison was performed using student t-test. * $p < 0.05$, ** $p < 0.01$, *** $p < 0.001$, and **** $p < 0.0001$ were considered as statistically significant difference compared to control.

study represents underlying mechanisms of acute promyelocytic leukemia (NB4 cell) and T-acute lymphocytic leukemia (MOLT-4 cell). In the future, using other leukemic cell lines such as chronic leukemic cells or B-acute lymphoblastic leukemia cells can provide valuable insight into the mechanisms of PG2 induced apoptosis mediated leukemic EV. Overall, our study demonstrated that PG2_EV influences CDK2, miR-339-5p and caspase-3, which are key apoptotic molecules, ultimately promoting apoptosis in acute leukemia.

Conclusion

Our recent study demonstrated the anticancer effect of the pomegranate-derived peptide PG2 on apoptosis via caspase-3, CDK2 and miR-339-5p mediated by extracellular vesicles in acute leukemia while exhibiting minimal effects on PBMCs. PG2 could be developed as a novel anticancer peptide for leukemia patients. Moreover, CDK2 and miR-339-5p from extracellular vesicles could be developed as alternative treatments for leukemia.

Methods

Pomegranate-derived peptide and daunorubicin

Pomegranate-derived peptides were synthesized from GeneScript with more than 96% purity. All the anticancer peptides used are shown in Table 1. Lyophilized pomegranate-derived peptide stock was stored at -20°C and dissolved in DMSO before use in experiments. Daunorubicin was purchased from TOKU-E, Bellingham, USA. Daunorubicin stock was stored at 4°C and dissolved in ultrapure water before use in experiments.

Leukemic cell culture and PBMC isolation

NB4 (acute promyelocytic leukemia) and MOLT-4 (T-acute lymphoblastic leukemia) cells were obtained from Cell Line Service GmbH (Eppelheim, Germany). The cells were cultured in RPMI-1640 medium supplemented with 10% fetal bovine serum (FBS) and 1% penicillin-streptomycin in a humidified incubator at 37°C with 5% CO_2 . The RPMI-1640 medium was replaced every 2–3 days.

All experimental protocols were carried out in accordance with relevant guidelines and regulations. Peripheral blood mononuclear cells isolation protocol was approved by Mahidol University Central Institutional Review Board (MU-CIRB). Informed consent was obtained from all subjects. Peripheral blood mononuclear cells (PBMCs) were isolated by the Ficoll-Hypaque method. (ethics approval no. MU-CIRB 2022/216.0808). Briefly, whole blood from healthy participants was diluted with PBS at a ratio of 1:1 and then gently overlaid

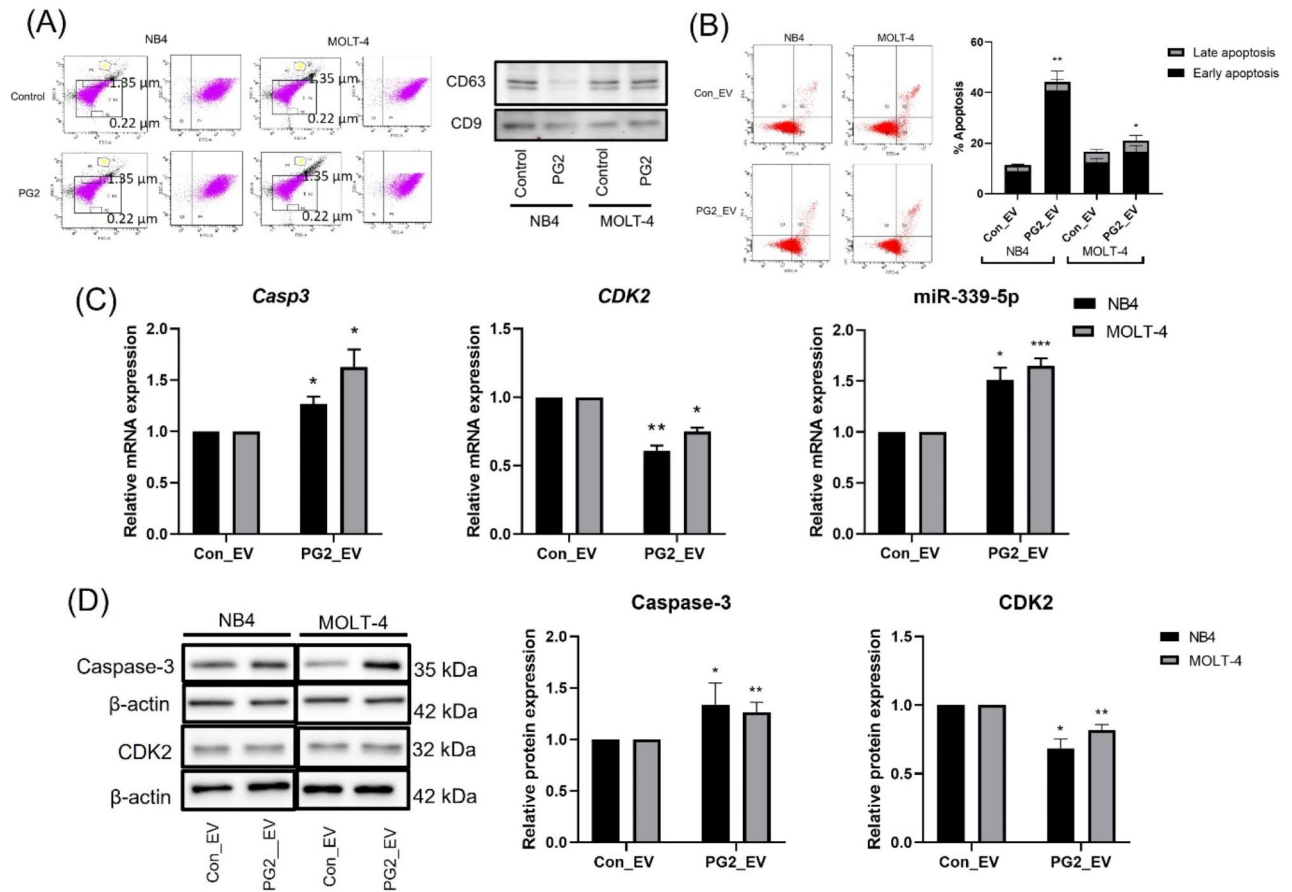


Fig. 6. Effect of PG2_EVs on caspase-3, CDK2 and miR-339-5p expression in NB4 and MOLT-4 cells. NB4 and MOLT-4 cells were triggered with 10 $\mu\text{g}/\text{ml}$ of PG2_EVs for 48 h followed by assessment of caspase-3, CDK2 and miR-339-5p expression using RT-qPCR and western blotting techniques. **(A)** Characterization of Con_EVs and PG2_EVs in the size range of 0.22–1.35 μm identified using Annexin V, CD9 and CD63 markers. **(B)** Flow cytometry scatter plot and percentage of apoptotic cells in PG2_EVs-treated NB4 and MOLT-4. **(C)** The relative mRNA expression of Casp3, CDK2 and miR-339-5p in PG2_EVs-treated NB4 and MOLT-4. **(D)** The relative protein expression of caspase-3 and CDK2 in PG2_EVs-treated NB4 and MOLT-4 cells. Data are represented as mean \pm S.E.M of three independent experiments. Statistical comparison was performed using student t-test. * $p < 0.05$, ** $p < 0.01$ and *** $p < 0.001$ were considered as statistically significant difference compared to Con_EVs.

diluted whole blood to Ficoll-Hypaque solution. After that, the mixture of blood and solution was centrifuged at 800 \times g for 20 min at 25 $^{\circ}\text{C}$. Then, the blood was washed with RPMI-1640 media twice, and the cell pellet was resuspended in RPMI-1640 media. PBMCs were counted by trypan blue staining in 96-well plates for MTT experiments.

MTT assay

To screen for anticancer peptides, NB4 and MOLT-4 cells were treated with 1000 $\mu\text{g}/\text{ml}$ anticancer peptides as shown in Table 1 for 24 h. Next, 15,000 NB4, MOLT-4 cells and 100,000 PBMCs were treated with PG2 at 500, 750 and 1000 $\mu\text{g}/\text{ml}$ for 24 h and 48 h in a 96-well plate, followed by incubation at 37 $^{\circ}\text{C}$ with 5% CO_2 . Afterward, 10 μl of 5 mg/ml MTT was added to each well. After 4 h of incubation, 100 μl of 10% SDS in 0.01 M HCl was added, and the mixture was then incubated overnight. Finally, the formazan crystal concentration was determined using a microplate reader at a wavelength of 570 nm (BioTek Instruments, Inc., Winooski, VT, USA). The half inhibitory concentration (IC₅₀) was calculated and used in further experiments.

Synergistic effect of PG2 and daunorubicin

NB4 and MOLT-4 cells were treated with 0.2 $\mu\text{g}/\text{ml}$ daunorubicin (TOKU-E, Bellingham, WA, USA), the IC₅₀ of PG2 or daunorubicin mixed with PG2 for 48 h. The viability of the NB4 and MOLT-4 cells was determined using MTT, as described previously. Three concentrations of PG2 and daunorubicin were required to calculate combination index (CI). The combination index (CI) value of combination between PG2 and daunorubicin was calculated using CompuSyn application.

Apoptosis assay

NB4 and MOLT-4 cells were treated with PG2 at the IC50 or with 10 µg/ml of PG2_EVs for 48 h. Subsequently, the cells were harvested and washed twice with PBS. Next, NB4 and MOLT-4 cells were stained with 3 µl of Annexin V-FITC conjugated with FITC (Biolegend, USA), 3 µl of 50 µg/ml propidium iodide (Sigma-Aldrich, Schnellendorf, Germany) and 1x Annexin V binding buffer (BD Biosciences, San Diego, CA, USA), followed by a 15-minute incubation in the dark. The apoptotic cells were then analyzed using a FACSCantoII flow cytometer.

Cell cycle assay

NB4 and MOLT-4 cells were treated with PG2 at the IC50 for 48 h. The cells were harvested, washed twice, and resuspended in PBS. NB4 and MOLT-4 cells were fixed with cold 70% ethanol for 30 min at 4 °C. After that, the cells were washed and then resuspended in PBS. Then, 100 µg/ml of RNase A (Roche, Basel, Switzerland) was added for 30 min at room temperature to remove RNA. Then, 50 µg/ml propidium iodide (Sigma-Aldrich, Schnellendorf, Germany) was added to stain the DNA for 10 min at room temperature in the dark. Finally, the cell cycle phases were analyzed using a FACSCantoII flow cytometer.

Prediction of target proteins and miRNAs in EVs by bioinformatic tools

PG2-responsive proteins were predicted by the SwissTargetPrediction application (<http://www.swisstargetprediction.ch/>). The LLKLFF and PFLKGT sequences from the PG2 whole sequence (LLKLFFPFLKGTG) were used as inputs for the prediction of target proteins. Next, the proteomic data of EVs from different cancer cell types³⁸ were used to predict the proteins associated with EVs using a Draw Venn diagram. Furthermore, a network of target proteins and representative proteins involved in apoptosis, including caspase-3 (CASP3), caspase-8 (CASP8), and caspase-9 (CASP9), was constructed using STRING.

The target miRNAs in EVs predicted from the target protein sequence were further assessed. The sequence (Ensembl) of the target protein was retrieved from the National Center for Biotechnology Information (NCBI). The target miRNAs were predicted by 3 tools, namely, miRDB (<https://mirdb.org/>), TargetScan (https://www.targetscan.org/vert_80/), and DIANA (<https://dianalab.e-ce.uth.gr/html/universe/index.php?r=microtv4>). In miRDB, the target score was set to more than 90. In TargetScan, the aggregate score (Pct) was set to more than 0.1. In DIANA, miTG was set to more than 0.9. All possible miRNAs in leukemic EVs were retrieved from the EVmiRNA database (<http://bioinfo.life.hust.edu.cn/EVmiRNA>)³⁹. Finally, the candidate miRNAs were chosen from 3 bioinformatic tools and EVmiRNAs.

Isolation and characterization of leukemic extracellular vesicles

NB4 and MOLT-4 cells were treated with PG2 at the IC50 for 48 h (PG2_EVs), and conditioned media were collected. Cells treated with 1% DMSO were used as the control group of extracellular vesicles (Con_EVs). First, the conditioned media were centrifuged at 300×g for 5 min to remove cells, and the supernatant was then centrifuged at 1500×g for 15 min to remove cellular debris. After that, the supernatant was centrifuged at 17,000×g for 30 min to pellet the EVs. The EV pellet was washed with PBS twice at 17,000×g for 30 min. Finally, EVs were dissolved in PBS and stored at -80 °C for further assessment.

Standard fluorescent polystyrene particles 0.22 µm and 1.35 µm in size were utilized to generate scatter plots aiding in the identification of extracellular vesicles (EVs). To characterize leukemic EVs, the suspended EVs were stained with FITC-Annexin V dissolved in 1x Annexin V binding buffer with counting beads (BD bioscience, Palo Alto, CA, USA). Moreover, CD9 and CD63 EVs were characterized by western blotting. The EV concentration was measured by the Bradford assay (Bio-Rad Laboratory, USA). Isolated EVs were used to treat acute leukemia cells for further study.

miRNA and gene expression by real-time polymerase chain reaction (RT-qPCR)

NB4 and MOLT-4 cells were treated with PG2 at the IC50 for 48 h or with 10 µg/ml PG2_EVs for 48 h. The cells were harvested and washed twice. RNA extraction was performed using GENEzol™ reagent according to the manufacturer's instructions (New England Biolab, Inc., Ipswich, MA, USA). The amount of extracted RNA was determined using a Nanodrop2000 spectrophotometer, and the RNA was subsequently converted to cDNA using a RevertAid First Strand cDNA Synthesis Kit (Thermo Scientific, Waltham, MA, USA). For miRNA analysis, the miRNA 1st-strand cDNA Synthesis Kit (Agilent Technologies, Santa Clara, CA, USA) was utilized to synthesize cDNA from RNA. Subsequently, cDNA was subjected to analysis using Luna real-time PCR mastermix (New England Biolab, Inc., Ipswich, MA, USA) along with designed primers. The analysis was carried out using a Bio-Rad CFX96 Touch™ real-time PCR system (Bio-Rad, Hercules, CA, USA) to quantify the threshold cycle (Ct) of the sample. The mRNA expression levels were calculated using the $2^{-\Delta\Delta CT}$ method, with GAPDH and U6 serving as the internal controls for mRNA and miRNA, respectively. The primers utilized in this study are listed in Table 2.

Apoptotic protein by Western blot analysis

NB4 and MOLT-4 cells were treated with PG2 at the IC50 for 48 h or with 10 µg/ml PG2_EVs for 48 h. The cells were collected and washed twice. RIPA lysis buffer supplemented with 1% protease inhibitor (Merck Millipore, Burlington, MA, USA) was used to lyse the cells, and the protein-containing cell lysates were harvested. The protein concentration of the cell lysate of leukemic cells was determined using a Dual-Range BCA Protein Assay Kit (Visual Protein, Taipei, Taiwan). Protein cell lysates were separated by SDS-PAGE. Proteins on SDS-PAGE gels were subsequently transferred to nitrocellulose membranes. After that, the nitrocellulose membrane was blocked with EveryBlot Blocking Buffer (Bio-Rad, Inc., Hercules, CA, USA) or 5% nonfat milk at room temperature and then incubated with primary antibodies against CD9, CD63 (Abcam Inc., Cambridge, UK), CDK2, caspase-3, and β-Actin (Cell Signaling Technology, Danvers, MA, USA) overnight at 4 °C. Next, the

Primers	Sequence
Caspase-3	F: 5'-TTCAGAGGGGATCGTTGTAGAAGTC-3' R: 5'-CAAGCTTGTTCGGCATACTGTTTCAG-3'
CDK2	F: 5'-TGGATGCCTCTGCTCTCACTG-3' R: 5'-GAGGACCCGATGAGAATGGC-3'
GAPDH	F: 5'-GCACCGTCAAGGCTGAGAA-3' R: 5'-AGGTCCACCCTGACACGTTG-3'
miR-339-5p	F: 5'-TCCCTGTCTCCAGGAGCTCACG-3'
U6	F: 5'-CTCGCTTCGGCAGCAC-3'

Table 2. The sequence of primers used in this study.

membrane was incubated with horseradish peroxidase (HRP)-conjugated secondary antibodies, including HRP-linked anti-mouse IgG (Cell Signaling Technology, Danvers, MA, USA) or HRP-linked anti-rabbit (Merck Millipore, Burlington, MA, USA). Finally, the band intensities in the membrane were detected by enhanced chemiluminescence (ECL) substrate (Bio-Rad, Inc., Hercules, CA, USA). The protein band intensity was calculated using Lab™ software (Bio-Rad, Inc., Hercules, CA, USA) and normalized to that of β -actin.

Statistical analysis

All experiments were conducted in triplicate, and the data were presented as the mean \pm standard error of the mean (S.E.M.). All the graphs were constructed using GraphPad Prism version 8.0 (GraphPad Inc., San Diego, CA, USA). Statistical analysis was performed using GraphPad Prism version 8.0. Student's t test was used to compare two groups. A p value < 0.05 was considered to indicate statistical significance.

Data availability

The datasets generated and/or analyzed during the current study are available in the GenBank repository, [Accession number: ENSG00000123374, <https://www.ncbi.nlm.nih.gov/gene/1017>]. Further information and requests for resources and reagents should be directed to and will be fulfilled by the Lead Contact Dalina Tanyong (dalina.itc@mahidol.ac.th).

Received: 13 June 2024; Accepted: 28 October 2024

Published online: 09 November 2024

References

- Siegel, R. L., Miller, K. D., Fuchs, H. E. & Jemal, A. Cancer statistics, 2022. *CA Cancer J. Clin.* **72**, 7–33. <https://doi.org/10.3322/caac.21708> (2022).
- Izuegbuna, O. Leukemia chemoprevention and therapeutic potentials: Selected medicinal plants with anti-leukemic activities. *Nutr. Cancer* **74**, 437–449. <https://doi.org/10.1080/01635581.2021.1924209> (2022).
- Zhang, Y., Wang, C., Zhang, W. & Li, X. Bioactive peptides for anticancer therapies. *Biomater. Transl.* **4**, 5–17. <https://doi.org/10.12336/biomatertransl.2023.01.003> (2023).
- Deesrisak, K. et al. Bioactive peptide isolated from sesame seeds inhibits cell proliferation and induces apoptosis and autophagy in leukemic cells. *EXCLI J.* **20**, 709–721. <https://doi.org/10.17179/excli2021-3406> (2021).
- Su, L. Y., Shi, Y. X., Yan, M. R., Xi, Y. & Su, X. L. Anticancer bioactive peptides suppress human colorectal tumor cell growth and induce apoptosis via modulating the parp-p53-mcl-1 signaling pathway. *Acta Pharmacol. Sin.* **36**, 1514–1519. <https://doi.org/10.1038/aps.2015.80> (2015).
- Subkorn, P., Norkaew, C., Deesrisak, K. & Tanyong, D. Punicalagin, a pomegranate compound, induces apoptosis and autophagy in acute leukemia. *PeerJ* **9** <https://doi.org/10.7717/peerj.12303> (2021). e12303.
- Deng, Y. et al. The extract from punica granatum (pomegranate) peel induces apoptosis and impairs metastasis in prostate cancer cells. *Biomed. Pharmacother.* **93**, 976–984. <https://doi.org/10.1016/j.biopha.2017.07.008> (2017).
- Dahlawi, H., Jordan-Mahy, N., Clench, M., McDougall, G. J. & Maitre, C. L. Polyphenols are responsible for the proapoptotic properties of pomegranate juice on leukemia cell lines. *Food Sci. Nutr.* **1**, 196–208. <https://doi.org/10.1002/fsn3.26> (2013).
- Kokilakanit, P., Koontongkaew, S., Roytrakul, S. & Utispan, K. A novel non-cytotoxic synthetic peptide, pug-1, exhibited an antibiofilm effect on streptococcus mutans adhesion. *Let. Appl. Microbiol.* **70**, 151–158. <https://doi.org/10.1111/lam.13265> (2020).
- Guo, G., Wang, H. X. & Ng, T. B. Pomegranin, an antifungal peptide from pomegranate peels. *Protein Pept. Lett.* **16**, 82–85. <https://doi.org/10.2174/092986609787049330> (2009).
- Mardani, R. et al. MicroRNA in leukemia: Tumor suppressors and oncogenes with prognostic potential. *J. Cell. Physiol.* **234**, 8465–8486. <https://doi.org/10.1002/jcp.27776> (2019).
- Son, S. W. et al. Participation of microRNAs in the treatment of cancer with phytochemicals. *Molecules* **25** <https://doi.org/10.3390/molecules25204701> (2020).
- Pando, A., Reagan, J. L., Quesenberry, P. & Fast, L. D. Extracellular vesicles in leukemia. *Leuk. Res.* **64**, 52–60. <https://doi.org/10.1016/j.leukres.2017.11.011> (2018).
- Chang, W. H., Cerione, R. A. & Antonyak, M. A. Extracellular vesicles and their roles in cancer progression. *Methods Mol. Biol.* **2174**, 143–170. https://doi.org/10.1007/978-1-0716-0759-6_10 (2021).
- Kreger, B. T., Johansen, E. R., Cerione, R. A. & Antonyak, M. A. The enrichment of survivin in exosomes from breast cancer cells treated with paclitaxel promotes cell survival and chemoresistance. *Cancers (Basel)* **8**. <https://doi.org/10.3390/cancers8120111> (2016).
- Jang, J. Y., Lee, J. K., Jeon, Y. K. & Kim, C. W. Exosome derived from epigallocatechin gallate treated breast cancer cells suppresses tumor growth by inhibiting tumor-associated macrophage infiltration and m2 polarization. *BMC Cancer* **13**, 421. <https://doi.org/10.1186/1471-2407-13-421> (2013).
- Chaurasiya, P. S. et al. Prevalence of acute myeloid leukemia and its associated risk factors at a tertiary care center: A retrospective cross-sectional study. *Ann. Med. Surg. (Lond)*. **85**, 4794–4798. <https://doi.org/10.1097/ms9.0000000000001189> (2023).

18. Rasaratnam, K., Nantasenamat, C., Phaonakrop, N., Roytrakul, S. & Tanyong, D. A novel peptide isolated from garlic shows anticancer effect against leukemic cell lines via interaction with bcl-2 family proteins. *Chem. Biol. Drug Des.* **97**, 1017–1028. <https://doi.org/10.1111/cbdd.13831> (2021).
19. Chatupheeraphat, C. et al. A novel peptide derived from ginger induces apoptosis through the modulation of p53, bax, and bcl2 expression in leukemic cell lines. *Planta Med.* **87**, 560–569. <https://doi.org/10.1055/a-1408-5629> (2021).
20. Chuang, C. M., Monie, A., Wu, A., Mao, C. P. & Hung, C. F. Treatment with ll-37 peptide enhances antitumor effects induced by cpg oligodeoxynucleotides against ovarian cancer. *Hum. Gene Ther.* **20**, 303–313. <https://doi.org/10.1089/hum.2008.124> (2009).
21. Ebrahimdoust, M., Hayati, H. M., Moghaddam, M. M. & Bahreini, M. A short cationic peptide derived from cecropin and melittin peptides induce apoptosis in jurkat and raji leukemia cell lines. *Protein Pept. Lett.* **30**, 477–485. <https://doi.org/10.2174/0929866530666230512142826> (2023).
22. Abd-Rabou, A. A., Shalby, A. B. & Kotob, S. E. Newly synthesized punicalin and punicalagin nano-prototypes induce breast cancer cytotoxicity through ros-mediated apoptosis. *Asian Pac. J. Cancer Prev.* **23**, 363–376. <https://doi.org/10.31557/apjcp.2022.23.1.363> (2022).
23. Moga, M. A. et al. Pharmacological and therapeutic properties of punica granatum phytochemicals: Possible roles in breast cancer. *Molecules.* **26** <https://doi.org/10.3390/molecules26041054> (2021).
24. Chiangjong, W., Chutipongtanate, S. & Hongeng, S. Anticancer peptide: Physicochemical property, functional aspect and trend in clinical application (review). *Int. J. Oncol.* **57**, 678–696. <https://doi.org/10.3892/ijo.2020.5099> (2020).
25. Shoombuatong, W., Schaduagrang, N. & Nantasenamat, C. Unraveling the bioactivity of anticancer peptides as deduced from machine learning. *Excli J.* **17**, 734–752. <https://doi.org/10.17179/excli2018-1447> (2018).
26. Tan, S. H. et al. Propofol suppressed cell proliferation and enhanced apoptosis of bladder cancer cells by regulating the mir-340/cdk2 signal axis. *Acta Histochem.* **123**, 151728. <https://doi.org/10.1016/j.acthis.2021.151728> (2021).
27. Zhang, C., Wang, X. & Zhang, C. Icaritin inhibits cdk2 expression and activity to interfere with tumor progression. *iScience.* **25**, 104991. <https://doi.org/10.1016/j.isci.2022.104991> (2022).
28. Sharifi, H. et al. Micronas and response to therapy in leukemia. *J. Cell. Biochem.* **120**, 14233–14246. <https://doi.org/10.1002/jcb.28892> (2019).
29. Li, Y. et al. Mir-339-5p inhibits metastasis of non-small cell lung cancer by regulating the epithelial-to-mesenchymal transition. *Oncol. Lett.* **15**, 2508–2514. <https://doi.org/10.3892/ol.2017.7608> (2018).
30. Feng, J. et al. Cross-talk between the Er pathway and the Incrna mafg-as1/mir-339-5p/cdk2 axis promotes progression of er + breast cancer and confers tamoxifen resistance. *Aging (Albany N Y)* **12**, 20658–20683. <https://doi.org/10.18632/aging.103966> (2020).
31. Hu, T. et al. Mir-339 promotes development of stem cell leukemia/lymphoma syndrome via downregulation of the bcl2l1 and bax proapoptotic genes. *Cancer Res.* **78**, 3522–3531. <https://doi.org/10.1158/0008-5472.Can-17-4049> (2018).
32. Wong, R. S. Y. Apoptosis in cancer: From pathogenesis to treatment. *J. Experimental Clin. cancer Research: CR* **30**, 87–87. <https://doi.org/10.1186/1756-9966-30-87> (2011).
33. Abbaszade Dibavar, M., Pourbagheri-Sigaroodi, A., Asemiani, Y., Salari, S. & Bashash, D. Extracellular vesicles (evs): What we know of the mesmerizing roles of these tiny vesicles in hematological malignancies? *Life Sci.* **271**, 119177. <https://doi.org/10.1016/j.lfs.2021.119177> (2021).
34. Yan, W. et al. Extracellular vesicles carrying mirna-181b-5p affects the malignant progression of acute lymphoblastic leukemia. *J. Transl. Med.* **19**, 511. <https://doi.org/10.1186/s12967-021-03174-w> (2021).
35. Luo, A. et al. Exosome-derived mir-339-5p mediates radiosensitivity by targeting cdc25a in locally advanced esophageal squamous cell carcinoma. *Oncogene* **38**, 4990–5006. <https://doi.org/10.1038/s41388-019-0771-0> (2019).
36. Taverna, S. et al. Curcumin modulates chronic myelogenous leukemia exosomes composition and affects angiogenic phenotype via exosomal mir-21. *Oncotarget* **7**, 30420–30439. <https://doi.org/10.18632/oncotarget.8483> (2016).
37. Huang, M. B., Wu, J. Y., Lillard, J. & Bond, V. C. Smr peptide antagonizes mortalin promoted release of extracellular vesicles and affects mortalin protection from complement-dependent cytotoxicity in breast cancer cells and leukemia cells. *Oncotarget* **10**, 5419–5438. <https://doi.org/10.18632/oncotarget.27138> (2019).
38. Hurwitz, S. N. et al. Proteomic profiling of nci-60 extracellular vesicles uncovers common protein cargo and cancer type-specific biomarkers. *Oncotarget* **7**, 86999–87015. <https://doi.org/10.18632/oncotarget.13569> (2016).
39. Liu, T. et al. Evmirna: A database of mirna profiling in extracellular vesicles. *Nucleic Acids Res.* **47**, D89–D93. <https://doi.org/10.1093/nar/gky985> (2019).

Acknowledgements

This research project is supported by Mahidol University. Funding source was no involvement in designing, collection, analysis, and interpretation of data.

Author contributions

K.C. designed experiments, conducted the study, analyzed the data, and wrote the manuscript. C.N. and M.N. conducted the study and analyzed the data. W.K. designed experiment. S.R. provided resources. D.T. designed experiments, approved the manuscript and provided resources. All authors reviewed the manuscript.

Declarations

Competing interests

The authors declare no competing interests.

Additional information

Supplementary Information The online version contains supplementary material available at <https://doi.org/10.1038/s41598-024-78082-2>.

Correspondence and requests for materials should be addressed to D.T.

Reprints and permissions information is available at www.nature.com/reprints.

Publisher's note Springer Nature remains neutral with regard to jurisdictional claims in published maps and institutional affiliations.

Open Access This article is licensed under a Creative Commons Attribution-NonCommercial-NoDerivatives 4.0 International License, which permits any non-commercial use, sharing, distribution and reproduction in any medium or format, as long as you give appropriate credit to the original author(s) and the source, provide a link to the Creative Commons licence, and indicate if you modified the licensed material. You do not have permission under this licence to share adapted material derived from this article or parts of it. The images or other third party material in this article are included in the article's Creative Commons licence, unless indicated otherwise in a credit line to the material. If material is not included in the article's Creative Commons licence and your intended use is not permitted by statutory regulation or exceeds the permitted use, you will need to obtain permission directly from the copyright holder. To view a copy of this licence, visit <http://creativecommons.org/licenses/by-nc-nd/4.0/>.

© The Author(s) 2024